The Effect of Layer Spacing Changes in the SmA Phase on Defects Observed in SSFLC Devices.

Chenhui Wang and Philip J. Bos[1]
Liquid Crystal Institute, Kent State University, Kent, Ohio 44242, USA
Satyendra Kumar
Department of Physics, Kent State University, Kent, Ohio 44242
Michael Wand and Mark Handschy
Displaytech Inc., Longmont, CO 80503, USA

Abstract

The effect of the temperature dependence of the smectic layer spacing in the smectic-A (SmA) phase on the formation of defects in the ferroelectric smectic-C (SmC*) phase is investigated with x-ray scattering technique. The study is based on thin parallel-aligned surface stabilized ferroelectric liquid crystal cells with two different alignment conditions, high pretilt SiO_x alignment and low pretilt polyimide films. It is found that defects observed in the SmC* phase have much more profound dependence on the layer changes and chevron formation in the SmA phase than in the SmC* phase. We find that thermal layer expansion with decreasing temperature in the SmA phase suppresses the formation of defects observed in the SmC phase.*

1. Introduction

Since surface stabilized ferroelectric liquid crystal (SSFLC) was first introduced by Clark and Lagerwall in 1980,[1] bistable ferroelectric liquid crystal displays have attracted a lot of attention for display application due to its fast response time, wide viewing angle, high contrast ratio and zero power consumption. It can be seen that in a nearly defect free SmC* device (free of zig-zag defects), some of the more subtle disruptions of the otherwise uniform SmC* structure can be observed first as the cell is cooled through the SmA phase during the cell preparation. For this reason, we consider that the defects found in the SmA phase are significant when considering a defect free SmC* device.

Unlike layer shrinkage and chevron formation in SmC that can be accommodated by director rotation, chevron formation in SmA will cause defects and these defects may alter the surface alignment and leave a remnant of a defect in SmC. More specifically, in SmC phase, as the layers contract due to the tipping of the director from the layer normal, a chevron forms, but defects are not necessarily seen. The reason for this is that in SmC phase, even though a chevron layer structure forms, it is possible for the director to rotate so that there is a continuous change in the director configuration across the chevron apex. Layer spacing changes are expected to be smaller in SmA phase, however the initiation of defects and non-uniformities can be much more noticeable. This is because if the layers contract, and a chevron structure is formed, the SmA structure cannot accommodate a chevron structure without the appearance of discontinuities in the director field.

In this paper we compare the layer spacing changes using high-resolution X-ray analysis and the defects observed for two materials, and for the case of low and high pretilt alignment in exploration for a defect free SSFLC device.

2. Experimental

Our studies were performed using sandwich type parallel aligned cells with the cell gap ~1μm. Both 5° obliquely evaporated SiO and polyimide PI2555 from Nissan were used as alignment layers. The SiO deposition took place in a high vacuum (10^{-6}-10^{-7} torr) bell jar at room temperature. The SiO boat was a multi-heat-baffled, tantalum boat. The incident angle is 5 degree (85 degree to the cell normal). The amount of silicon oxide evaporated during the deposition was monitored by an Inficon XTM/2 deposition monitor using a sensor-crystal (Gold, 6 MHz), which is situated directly above the boat. The substrates were located about 73cm from the source. The deposition rate is about 2-5Å/sec. The final SiO thickness is about 250Å calibrated by an ellipsometer. PI2555 was spin coated on the glass substrate and hard baked at 270°C for one hour. The polyimide coated substrate was then rubbed with velvet cloth. The pretilt angles for SiO alignment and PI2555 alignment are 34 degree and <1 degree respectively measured with magnetic null method. The cell is assembled with parallel alignment. The FLC was filled at isotropic state in vacuum and cooled down very slowly (<2°C/min) to room temperature. The FLCs we used in the experiments are Felix-019-000 and Felix-019-100 from Clariant. Their physical properties are shown in Table 1.

Table 1 Table 1. Physical Properties of Felix-019-000 and-100

Properties	Felix-019-000 (F000)	Felix-019-100 (F100)
Phase sequence	SmC^* 60.8 S_A 76.5 N^* 82-81 I	SmC^* 67.2 S_A 81.5 N^* 88.5 I
P_s (nC/cm^2)	8.3	39

[1] Email: pbos@kent.edu

To investigate layer structure, high resolution X-ray diffraction studies were carried out at Argonne National Lab using μ-CAT station (beam size 200μm by 0.5mm) for both high pretilt and low pretilt alignment cells. To reduce the absorption of X-ray, thin glass plates with a thickness of about 60μm were used to make the cells. A temperature controller is used to keep the temperature variation of the sample within ±0.1 K. After performing the 2-θ scans to determine the smectic layer spacing, the detector was set at 2θ angle to receive the diffracted beam. The θ-scans were then performed, which involve sample rotations by angle θ, to determine the details of the chevron structure.

3. Results and Discussion

3.1 Defects other than Zigzags

5° SiO deposition method normally generates uniform high pretilt alignment with the director lying parallel to the evaporation direction. Geometrically, a zigzag free C1 structure can be achieved with 5° obliquely evaporated SiO alignment[7,8,9]. However, this device still generally shows some subtle defects[10,11], such as those reported before, are seen also in the SmA phase. One defect we found in our SiO aligned cell is the pin defect (Figure 1), which is related to the spacers and the dust, and it looks like a meteor.

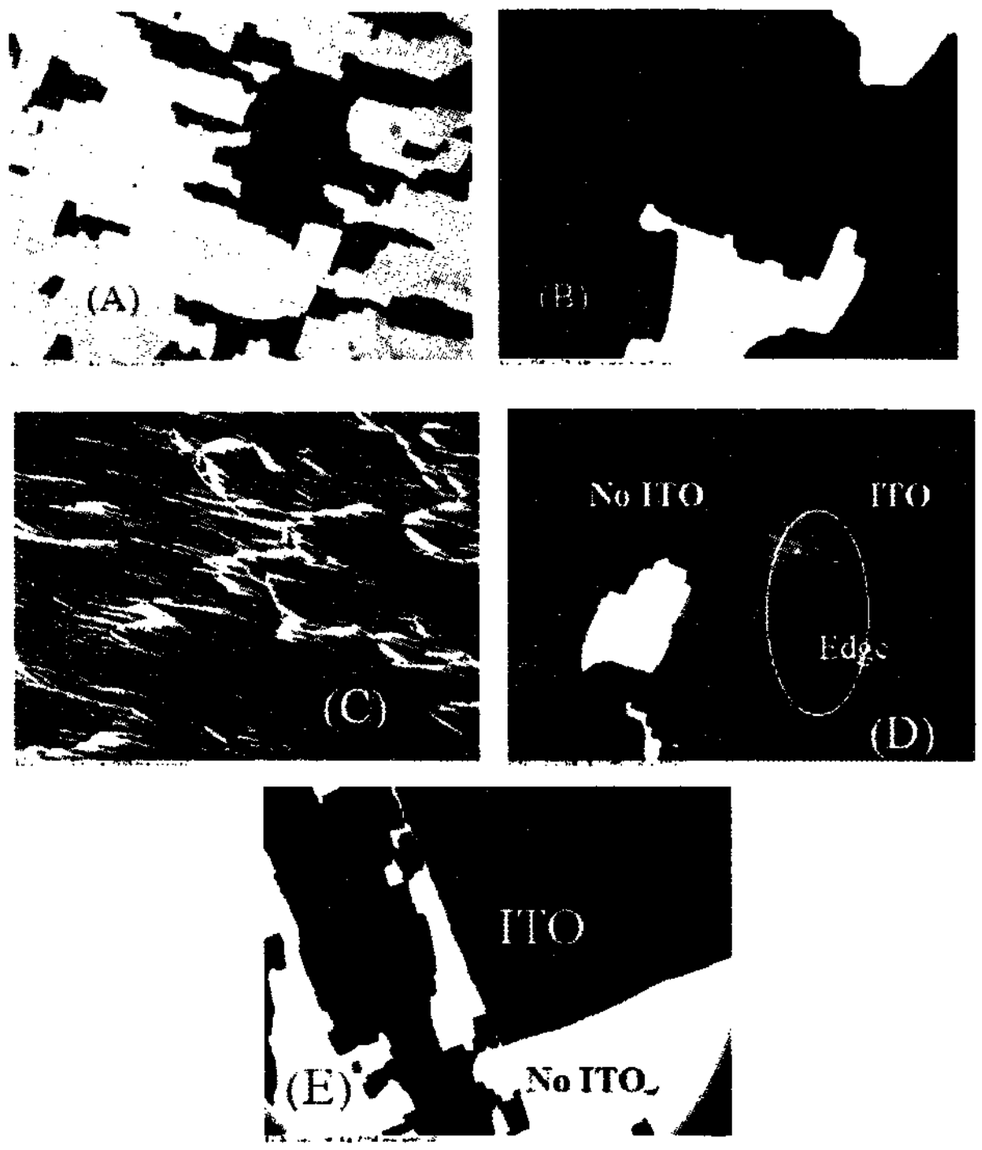

Figure 1 The microscopic textures of the cells with and without spacers in room tempeture of SmC. For Felix-019-000: (A) The cell with spacers, (B) Spacer in glue edge only; For Felix-019-100: (C) The Pin defects around the spacers, (D) Pin defects around unevenly etched ITO edge. (E) The total defect-free texture around the pixel edge after optimizing the etching condition and putting spacers in glue edge only.

We found that the top of the pin defect is a dust particle or a spacer and the tail of this pin defects is always along the alignment direction. And this pin defect was originally coming from SmA. (Figure 2)

Figure 2 Pin defect in SmA phase under the crossed polarizer microscope

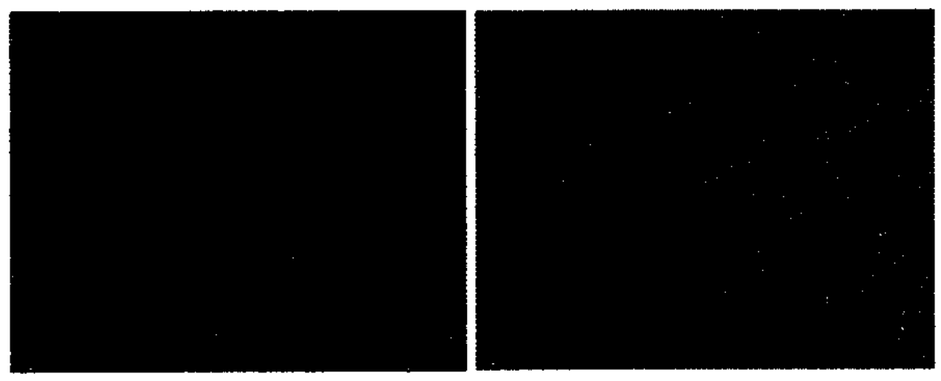

Figure 3 Layer undulation defect in the dark state in SmC* (Right) and SmA (Right) for F100 under the crossed polarizer microscope

In our case, we found that the F000 is not very sensitive to the presence of spacers. On the other hand, the spacers cause a lot of pin and focal conic defects for F100. Even the rough ITO etching edge can cause the pin defect. We eliminated this defect by mixing the spacers in the UV-curable glue instead of spraying spacers onto the entire substrate and properly controlling the etching condition. The pin defects are removed and the contrast ratio was improved significantly[10]. The textures of the cell before and after removing the spacers from the pixel region for both materials are also shown in Figure 1.

On the other hand, sometimes we can see subtle defects such as "layer undulation" defects in the dark state (Figure 3) for F100 in both SmA and SmC phases with SiO alignment, which indicates the high elastic strain of the layer.

3.2 X-ray scattering studies

To keep the cell gap uniform, so that pin defects would not be nucleated, the density of the spacer inside the cells for X-ray diffraction studies was kept very low. Figure 4 illustrates the rocking curves obtained while cooling the F100 from isotropic state to smectic A and then smectic C* state for both alignment. From the temperature vs. layer tilted angle relation shown in the top of Figure 5, we can see that the chevron structure was already formed in SmA for F100 with a high pretilt. And also the layer tilted angle increase with the decrease of the temperature. On the

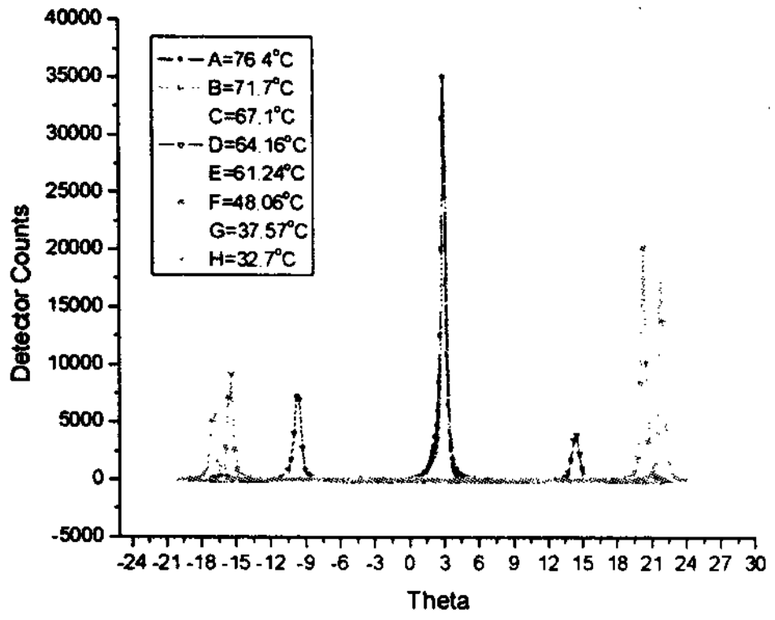

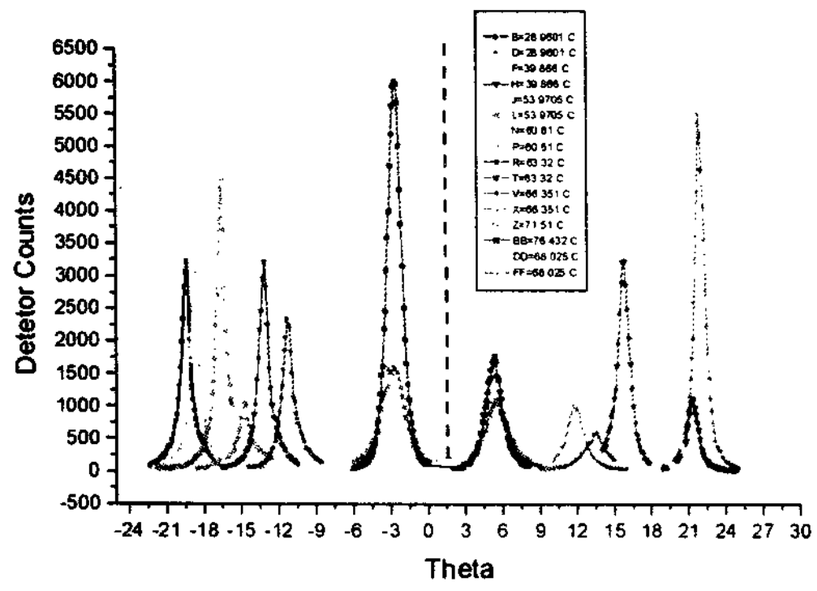

Figure 4 The rocking curves of θ–scan for F100 during the cooling with PI2555 (Top) and SiO alignment (Bottom).

other hand, the layer still keeps bookshelf like structure after the N* to SmA transition for low pretilt alignment. and then changes to chevron during the SmA-SmC transition. This indicates that the chevron formation in SmA may due to the high pretilt and layer shrinkage in SmA.

F000 has the similar rocking curve as F100 with SiO alignment. But instead of increasing the layer tilted angle in SmA, the tilted angle of F000 in SmA shrinks due to the layer expansion in SmA with the decreasing of the temperature (Figure 5 (C) (d) and Figure 6). Also the tilted angle of F000 in SmA is much smaller than that of F100. which maybe the reason why the pin defects was originally formed in SmA and also F100 is very sensitive to spacers and dust.

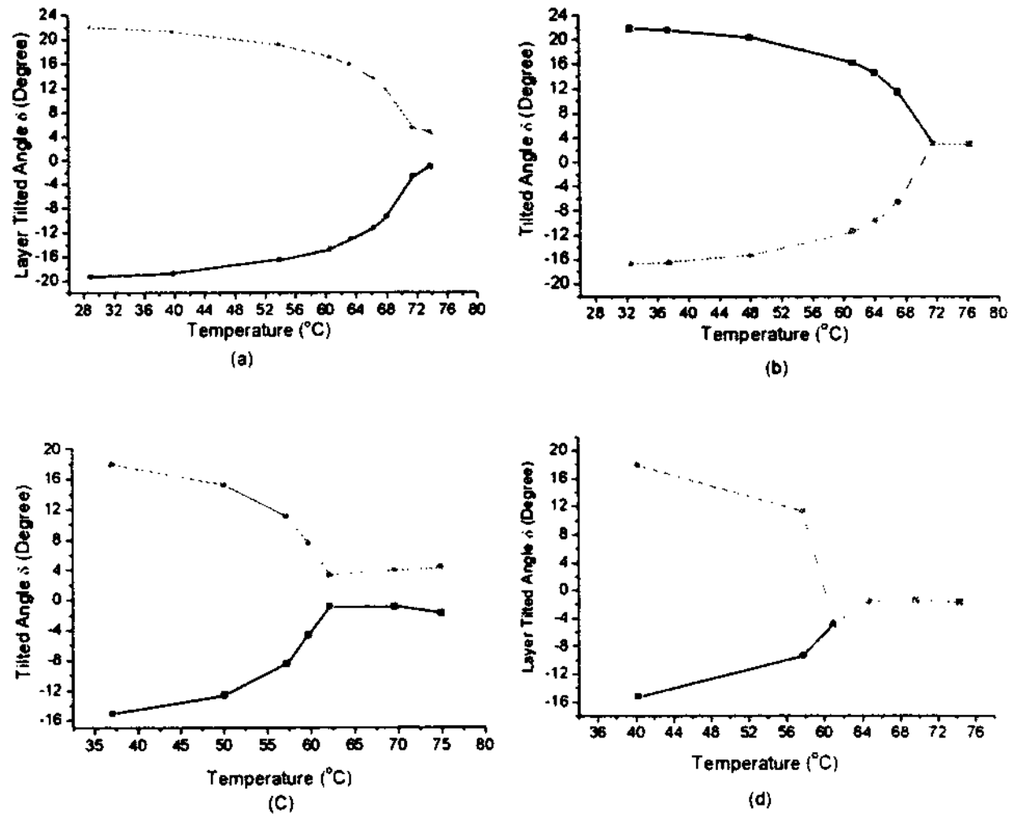

Figure 5 Layer tilted angle vs. temperature for F100 with SiO alignment (a) and PI2555 alignment (b); Bottom: Layer tilted angle vs. temperature for F000 with SiO alignment (c) and PI2555 alignment (d)

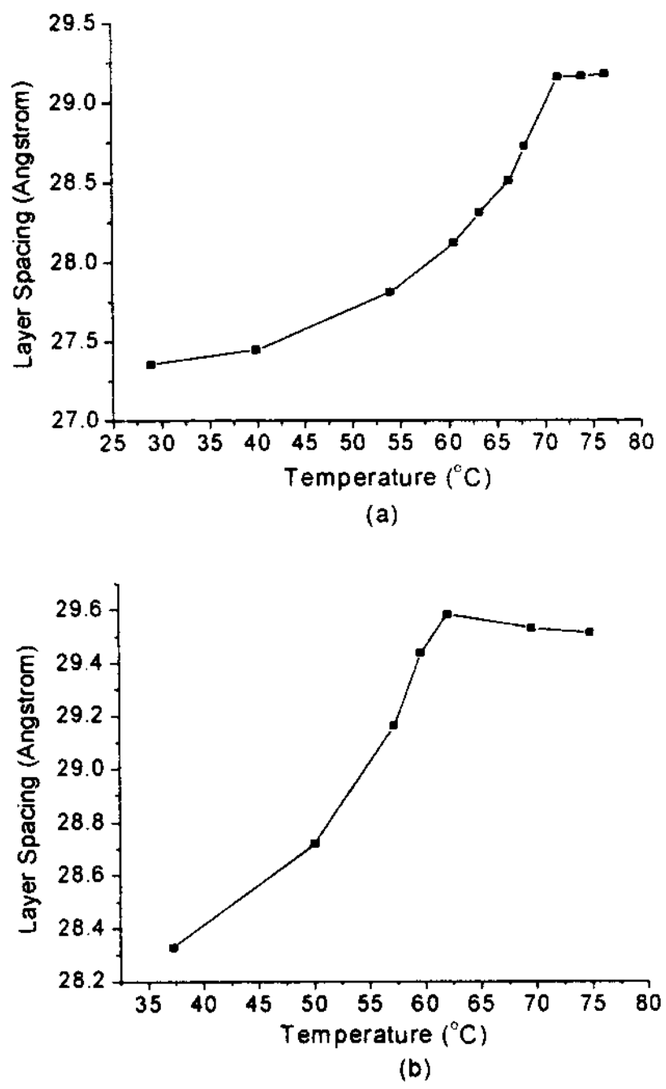

Figure 6 Layer spacing vs temperature for F100 (a) and F000 (b)

3.3 EO characteristic

The cells we used for EO measurement only have spacers in the glue edge. The contrast ratio is measured with reflective configuration under the crossed polarizer microscope with incandescent light and IR filter. The objective lens has numerical aperture of 0.25. The cell size is about 0.5'x1'. Fig. 7 and Fig. 8 show electrooptical properties of prepared SSFLC cells. Both cells have good bistability with high contrast ratio. Fig. 7 shows the voltage dependence of bistability of Felix-019-000 at 25°C. The cell gap is ~0.7μm. We measured its reflectance under the polarized microscope with 100Hz, 400μs pulse waveform. The cell shows very good bistability and contrast ratio (> 250:1). The memory angle $2\theta_{mem}$ is about 38 degree with zero field and switching angle is about 40 degree with field. The critical uniform latching voltage is around 8.5 volts for 0.7μm cell gap. If voltage supply is higher than 23 volts, the minimum pulse width is below 100μs. we can expect line time is less than 300μsec by using 3-phase waveform and full page addressing can be achieved under 0.3sec. This makes it a very promising candidate for electronic paper application. On the other hand, Felix-019-100 shows very promising results. Fig. 8 shows the pulse width dependence of bistability of Felix-019-100. The cell gap is ~0.8μm. From Fig.8, we can see that the cell can be uniformly latched even with 5V/μm, 100Hz, 250μs pulse width at room temperature. The zero-field memory angle $2\theta_{mem}$ is about 41 degree. And the contrast ratio is more than 700:1. The cell shows permanent bistability. At 45°C, the cell can be latched with 5V/μm, 100Hz, 70μs pulse width and $2\theta_{mem}$=36°. The low driving voltage and very high contrast ratio makes it highly desirable for potential LCoS application and can be used for normal LCoS microdisplay backplane, which is a CMOS VLSI chip providing ±2.5 V across each picture element.

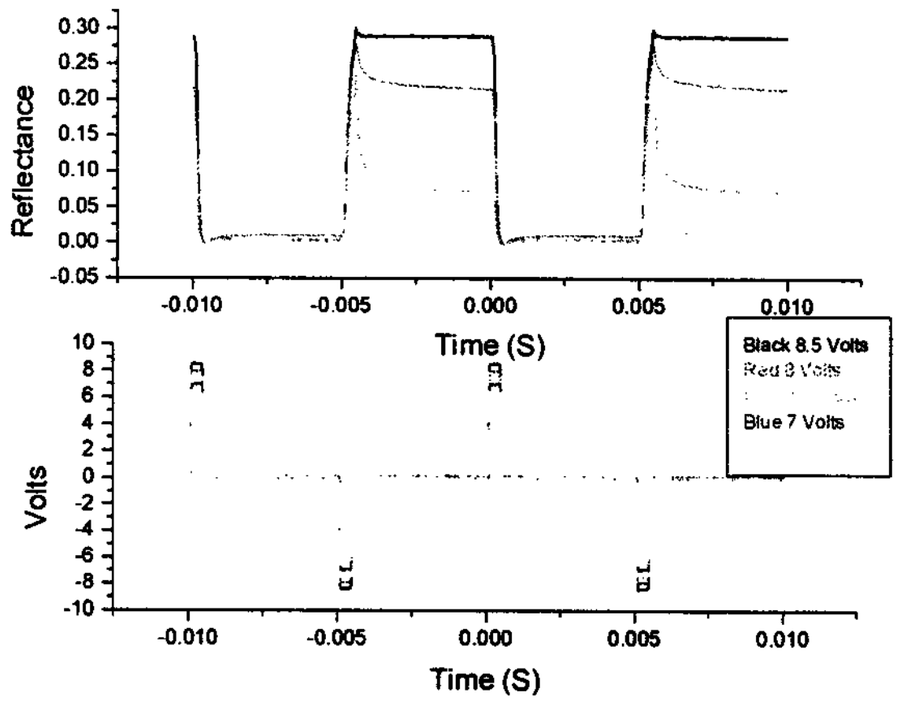

Figure 7 Voltage dependence of bistability for Felix-019-000 at 25°C (100 Hz, 400μs, Cell gap=0.7μm)

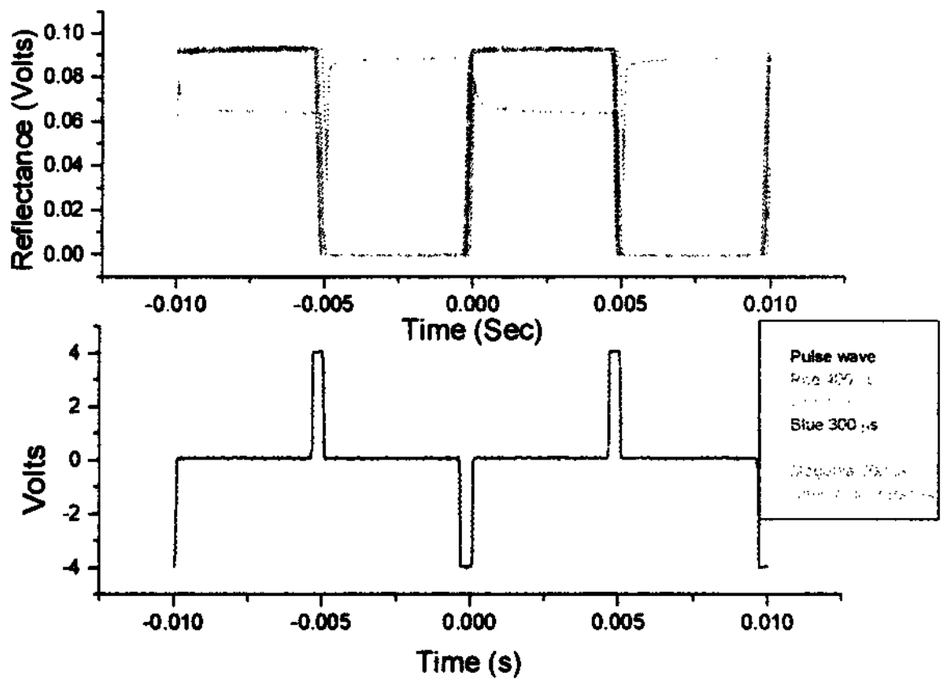

Figure 8 Pulse width dependence of bistability for Felix-019-100 at 25 °C (5V/Λμm, 100Hz, cell gap=0.8μm)

4. Conclusion

Temperature dependence of the smectic layer structure for F000 and F100 was studied by high resolution X-ray diffraction analysis. We found that due to the large pretilt angle of SiO alignment, the chevron already starts from SmA. And the layer thinning in SmA can also form the chevron structure. The layer shrinkage and chevron formation in the SmA are expected to necessitate defect formation. It will be easier to nucleate defects (such as pin defect or focal conic defects) around spacers. Unlike chevron formation in SmC that can be accommodated by director rotation; in SmA layer shrinkage and chevron formation will cause defects and these defects may alter the surface alignment and leave a remnant of a defect in SmC. On the other hand, layer expansion in SmA will have the opposite effect, in that the defects will be pushed out and a uniform layer structure is preferred. The fact that the pin defect already starts from SmA around the spacers with SiO alignment may relate to the chevron structure in SmA. The larger the layer tilted angle in SmA, the easier it is to form defects. In our case, F100 has twice the tilted angle than F000 in SmA. The layer and tilt angle of F000 decrease with the decreasing temperature, which may be the reason why F000 is not sensitive to the spacers.

Furthermore, we propose that if the material has layer expansion in SmA, it will actually stand up the layer and make the layer tilted angle in SmA smaller or even disappear. In this case, it will decrease the chance of defect formation.

5. Acknowledgements

We would like to acknowledge Displaytech Inc. for the financial support and also NSF ALCOM grant, DMR 89-20147 for the equipment. We would also thank Argonne National lab MU-CAT.

6. References

[1] N.A. Clark and S.T. Lagerwall. Appl. Phys. Lett. 36. 899-901 (1980).

[2] T. P. Rieker, N. A. Clark. G. S. Smith. D. S. Parmar. E. B. Sirota. and C. R. Safinya. Phys. Rev. Lett. 59. 2658 (1987).

[3] L. Taylor. R. M. Richardson. J. Ebbutt. and J. C. Jones. Mol. Cryst. Liq. Cryst. 263. 255 (1995)

[4] S. A. Jenkins. J. C. Jones. P. E. Dunn. S. D. Haslam. R. M. Richardson. and L. Taylor. Mol. Cryst. Liq. Cryst. 329. 19 (1999)

[5] G. Srajer. R. Pindak. and J. Patel. Phys. Rev. A 43. 5744 (1991).

[6] Y. Ouchi. J. Lee. H. Takezoe. A. Fukuda. K. Kondo. T. Kitamura. and A. Mukuh. Jpn. J. Appl. Phys.. Part 2 27. L725 (1988).

[7] J. Kanbe. H. Inoue. A. Mizutome. et. al., Ferroelectrics 114. 3-26 (1991).

[8] P.J. Bos. Japan Display'92. 523 (1992)

[9] P. J. Bos and K. R. Koehler/Beran. Ferroelectrics 85. 15-24 (1988)

[10] C. Wang. P. J. Bos. M. Wand and M. Handschy. SID'02 34-37 (2002)

[11] J. Xue. Ph. D thesis. University of Colorado. Boulder. USA (1989)